REPORT DOCUMENTATION PAGE

Form Approved
OMB No. 0704-0188

1. REPORT DATE *(DD-MM-YYYY)*	2. REPORT TYPE	3. DATES COVERED *(From - To)*
30-09-2006	Final Report	1 June 2006 – 30 Sept. 2006

4. TITLE AND SUBTITLE
Experimental and Numerical Characterization of Polymer Nanocomposites for Solid Rocket Motor Internal Insulation

5a. CONTRACT NUMBER

5b. GRANT NUMBER
FA9550-06-1-0356

5c. PROGRAM ELEMENT NUMBER

6. AUTHOR(S)
Koo, J. H., and Ezekoye, O. D.

5d. PROJECT NUMBER

5e. TASK NUMBER

5f. WORK UNIT NUMBER

7. PERFORMING ORGANIZATION NAME(S) AND ADDRESS(ES)
The University of Texas at Austin, Dept. of Mechanical Engineering, 1 University Station, C2200, Austin, TX 78712-0292

8. PERFORMING ORGANIZATION REPORT NUMBER

9. SPONSORING / MONITORING AGENCY NAME(S) AND ADDRESS(ES)
Dr. Charles Y-C Lee
AFOSR/NL
875 N. Randolph St., Ste. 325
Arlington, VA 22203

10. SPONSOR/MONITOR'S ACRONYM(S)
AFOSR

11. SPONSOR/MONITOR'S REPORT
AFRL-OSR-VA-TR-2013-0931

12. DISTRIBUTION / AVAILABILITY STATEMENT
Approved for public release; distribution unlimited

20130918362

13. SUPPLEMENTARY NOTES

14. ABSTRACT The objective of this research is to develop a modeling framework for simulating the insulative behavior of thermoplastic polyurethane elastomer nanocomposites (TPUNs) for solid rocket motors (SRMs) and the creation of software capable of predicting the properties of these TPUNs. This research combines numerical modeling and experimental characterization of TPUNs for SRM insulation. The TPUN thermophyscial properties and kinetic parameters will be characterized using thermogravimetric analysis, Multi-Function Sensor (MFS), and other thermal analyses. Numerical techniques for small scale physics from molecular dynamics (MD) simulations through population balance methods will be used to gain insight and intuition on the interactions between the polymeric and inorganic materials. These insights will help us to develop macroscopic kinetic models/descriptions in macroscale continuum models. These models will be first exercised against thermogravimetric and the MFS data, then small scale experiments using the LHMEL facility, and mesoscale experiments using AFRL Pi-K and Bates SRM firings. We formulated a simple non-charring ablation model, and then used it to perform a sensitivity analysis of failure time to four thermophysical properties. We found that failure time is most sensitive to the density and the heat of ablation, and is relatively insensitive to the thermal conductivity of the material. We reviewed numerical modeling of thermal protection materials literature, processed selective TPUNs, and calibrated a radiant heat apparatus to test TPUNs.

15. SUBJECT TERMS Ablation Modeling, Solid Rocket Motor Internal Insulation, Polymer Nanocomposites, Nanophase, Thermoplastic Elastomer, EPDM Rubber, Surface Modified MMT Clay, Carbon Nanofibers

16. SECURITY CLASSIFICATION OF:			17. LIMITATION OF ABSTRACT	18. NUMBER OF PAGES	19a. NAME OF RESPONSIBLE PERSON
a. REPORT	b. ABSTRACT	c. THIS PAGE			Joseph H. Koo
U	U	U	U	28	19b. TELEPHONE NUMBER *(include area code)* (512) 589-4170

TABLE OF CONTENTS

Section **Page No.**

Executive Summary.....1

1. Introduction.....3

2. Technical Program Summary.....3

3. Program Work Plan.....4

3.1 First Year Program Tasks.....5

3.2 Second Year Program Tasks.....6

3.3 Third Year Program Tasks.....7

4. Description of Polymer Nanocomposites.....7

4.1 Thermoplastic Elastomer.....7

4.2 Montmorilonite Nanoclays.....7

4.3 Carbon Nanofibers.....8

4.4 Ablation of TPUNs.....9

4.5 Microstructural Analyses of TPUNs.....9

5. Discussion of Results.....10

5.1 Review Paper.....10

5.2 Experimental Progress.....11

5.3 Numerical Progress.....13

5.4 Publications.....23

6. Summary and Future Plan.....24

6.1 Experimental.....24

6.2 Numerical.....24

7. References.....25

Acknowledgement.....27

Executive Summary

Research Objective

The objective of this research is to develop a modeling framework for simulating the insulative behavior of thermoplastic polyurethane elastomer nanocomposites (TPUNs) for solid rocket motors (SRMs) and the creation of software capable of predicting the properties of these TPUNs.

Research Approach

The proposed research combines numerical modeling and experimental characterization of TPUNs for SRM insulation. The TPUN thermophyscial properties and kinetic parameters are to be found using thermogravimetric analysis, Multi-Function Sensor (MFS) gauges, and other thermal analysis techniques. Numerical techniques for small scale physics from molecular dynamics (MD) simulations through population balance methods will be used to gain insight and intuition on the interactions between the polymeric and inorganic materials. These insights will help us to develop macroscopic kinetic models/descriptions which can be embedded in macroscale continuum models. These models will be first exercised against the thermogravimetric data and data generated from the MFS gauges. Subsequently, small scale experiments using the LHMEL facility with known heating conditions and well-controlled experiments will be conducted to provide us with data to further validate the numerical code. The numerical code and model will also be validated with mesoscale experiments using AFRL Pi-K and Bates SRM firings. Once this code is validated, numerical experiments with the code will help us to design optimized compositions (e.g., TPU and/or nanoparticles) of new TPUNs.

Scientific Relevance

The mechanisms through which the addition of nanoparticles modifies the decomposition of thermoplastic elastomers are not fully understood. One promising method for understanding these mechanisms is through the use of MD simulations. Because of the time scales over which MD simulations must be conducted, it has not been obvious how to incorporate MD findings into continuum type simulations. During our studies it is anticipated that a critical scientific breakthrough can occur if we are able to develop a mechanistic description of the polymer-inorganic material coupling process that can reside in a continuum code. One approach that has merit is a population balance (notional particle) description of the polymer and inorganic material distributions. In population balance treatment of aerosols, kinetics of breakage and coalescence are often included in continuum codes. There is a striking analogy between polymer bond breakage and subsequent capture by nanoparticles and aerosol aggregate breakage and subsequent capture by a scrubber particle. Our ability to create a continuum kinetic description of the MD physics would result not only in an important scientific contribution but also facilitate the Air Force's identification and design of new and future compositions for SRM insulation materials.

Progress

This report summarizes the first four months of our research effort from June 1 to Sept. 30, 2006. For this period of performance, we summarized a simple model for non-charring ablation, and then used that model to perform a sensitivity analysis of failure time based on four thermophysical properties. We found that failure time is most sensitive to the density and the heat of ablation of the material. It was also found that failure time is relatively insensitive to the

thermal conductivity of the material. These results indicate that improving the heat of ablation capacity of an ablative material should be the focus of future research.

We also reviewed numerical modeling literature for thermal protection materials, processed selective TPUN formulations for material characterization, and calibrated a radiant heat panel apparatus to conduct low heat flux experiments using the TPUNs. A user proposal entitled, "Thermophysical Properties Characterization of Thermoplastic Elastomer Nanocomposites" was approved by Oak Ridge National Laboratory/High Temperature Materials Laboratory (ORNL/HTML). This allows us to use their unique material characterization equipment and expertise to train our graduate students to conduct thermophysical property measurements of our TPUNs.

Personnel Supported

Morgan Bruns	PhD student, Mechanical Engineering
Dave Ho	MS student, Mechanical Engineering
Ofodike A. Ezekoye, Ph.D, P.E.	Professor, Mechanical Engineering
Joseph H. Koo, Sc.D.	Senior Research Fellow, Mechanical Engineering

Publications

1. Koo, J. H., D. W. Ho, and O. A. Ezekoye, "A Review of Numerical and Experimental Characterization of Thermal Protection Materials – Part I. Numerical Modeling", Paper AIAA-2006-4936, *42nd AIAA/ASME/SAE/ASEE Joint Propulsion Conference*, Sacramento, CA, July 9-12, 2006.
2. Ho, D. W., M. Bruns, J. H. Koo, and O. A. Ezekoye, "A Review of Numerical and Experimental Characterization of Thermal Protection Materials - Part II. Material Properties Characterization," submitted for presentation at the *48th AIAA/ASME/ASCE/AHS Structures, Structural Dynamics, and Materials Conference*, Waikiki, HI, Apr. 23-26, 2007.
3. Ho, D. W., M. Bruns, J, H. Koo, and O. A. Ezekoye, "A Review of Numerical and Experimental Characterization of Thermal Protection Materials - Part III. Experimental Testing," submitted for presentation at the *43rd AIAA/ASME/SAE/ASEE Joint Propulsion Conference*, Cincinnati, OH, July 8-11, 2007.
4. Nguyen, K., J. H. Koo, D. W. Ho, M. Bruns, and O. A. Ezekoye, "Experimental Characterization of Thermoplastic Elastomer Nanocomposites under Simulated Fire and Solid Rocket Motor Environments," submitted for presentation at the *43rd AIAA/ASME/SAE/ASEE Joint Propulsion Conference*, Cincinnati, OH, July 8-11, 2007.

1. Introduction

Insulation materials are required to protect solid rocket motor (SRM) cases against hostile combustion gaseous products generated in the rocket chamber. Various internal system components must be protected from extreme flow temperatures of 1,000 to 4,000°C and highly abrasive particles ejected at velocities greater than 1km/s. Kevlar®-filled ethylene-propylene-diene rubber (EPDM) is the baseline insulation material for solid rocket motor cases. A novel class of insulation materials was developed by the Air Force Research Laboratory that is lighter, exhibits better erosion and insulation characteristics and possesses a more cost-effective manufacturing process than the current baseline material.[1-5] We propose to develop a comprehensive numerical and experimental research program to understand the ablation and heat transfer characteristics of this new class of thermoplastic elastomer nanocomposites to facilitate the Air Force's identification and design efforts for new and future components of SRM insulation materials.

Koo *et al.*[6-8] have investigated different types of nanoparticles besides MMT nanoclays with phenolic resole resin for nozzle ablative material. These nanostructured materials exploit the ablation resistance of both resin and nanoparticles. The objective of this study was the development of a new class of nanostructured materials that are lighter and have better erosion and insulation characteristics than current ablatives for rocket nozzle assembly. Borden Chemicals' SC-1008, a phenolic resole, was selected as the resin. Several nanoparticles such as Southern Clay Products (SCP) nanoclay, Applied Sciences carbon nanofibers (CNFs), and Hybrid Plastics POSS® were evaluated with the SC-1008 phenolic resin. Based on wide-angle x-ray diffraction (WAXD) and transmission electron microscopy (TEM), selected nanoparticles were identified for further study. Cytec Engineered Materials (CEM) fabricated several MX-4926 alternates by replacing the carbon black filler with the selected nanoparticles for ablation testing. These polymer nanocomposites demonstrated significantly improved ablation and insulative performance versus the baseline ablative.[6-8]

A subscale solid rocket Char motor developed by AFRL/PRSM was used to study the ablation characteristics of the insulation materials.[1-5] Testing insulative or ablative materials in full-scale firings is not only expensive, but also requires lengthy planning and limited exposure time. Thus reducing the number of samples and the variety of test conditions available is a worthwhile endeavor. The Char motor has been shown to be a cost-effective, "fast turnaround" device to evaluate different insulative materials under identical conditions for initial material screening and development. Physical, mechanical, and thermophysical properties of these novel polymer nanocomposites have been determined and compared with baseline materials.[2]

2. Technical Program Summary

During the first year of the three-year program, processing of selective TPUNs in collaboration with AFRL/PRSM will be conducted. Multi-Function Sensor (MFS) gauges using TPUNs will be designed and fabricated. Characterization experiments to understand the degradation physics of these TPUNs will be conducted. TPUNs thermophysical properties and kinetic parameter will be determined. Molecular dynamics (MD) simulation of representative systems will be evaluated to gain insight into the role of nanoparticles on polymer chain stability. Phenomenological models using experimental data, MD results, and literature will be developed.

Requirements of TPUN thermal degradation computational tools will be determined. Research progress will be documented in a first year progress report.

Under year-two funding, a numerical code will be developed. Validation experiments with small scale degradation physics using the AFRL LHMEL facility will be performed. LHMEL data will be used to test numerical code. Validation experiments at mesoscales will be carried out using AFRL/PRSM's 2-lb Pi-K SRM firings in collaboration with AFRL personnel. The emerging new code will be used to conduct sensitivity tests. We will participate in designing the AFRL 15-lb Bates motor case with heat flux and MFS gauges to collect ablation data for the new TPUNs. Processing of new TPUNs in collaboration with AFRL will be accomplished. Thermophyscial properties and kinetic parameters for the new TPUNs will be measured. MFS gauge for new TPUNs will be fabricated. Research progress will be documented in a second year progress report.

Year-three funding will be used to refine the numerical code using validation experiments of small scale degradation physics of the new TPUNs using the LHMEL facility. Validation experiments of the mesoscale 15-lb Bates SRM with collaboration with AFRL will be conducted and data analyzed. A user's manual for the new code will be developed with sample cases. Research progress for the entire program will be documented in a final report.

3.0 Program Work Plan

A chronological list of program tasks by program years and a program schedule is listed in Table 1. Key research challenges involved in the proposed research are discussed below.

Table 1 Milestone for the Experimental and Numerical Characterization of Polymer Nanocomposites for Solid Rocket Motor Internal Insulation Research Program

Task Description	Fisrt Year				Second Year				Third Year			
First Year Tasks	Q1	Q2	Q3	Q4	Q5	Q6	Q7	Q8	Q9	Q10	Q11	Q12
Task 1 - Process Selective TPUNs	X											
Task 2 - Design & Fabricate MFS Gauge with TPUN	X	X										
Task 3 - Conduct Characterization Expts	X	X	X									
Task 4 - Determine TPUN Properties & Kinetics		X	X									
Task 5 - Develop Phenomenological Models	X	X	X	X								
Task 6 - Determine Reqs of TPUNTD Computational Tool			X	X								
Task 7 - First Year Progress Report/Technical Papers				X								
Second Year Tasks												
Task 8 - Implement Numerical Code					X	X						
Task 9 - Perform Validation Expts Using LHMEL						X						
Task 10 - Test Code with LHMEL Data							X	X				
Task 11 - Perform Validation Expts Using Pi-K Motor						X	X					
Task 12 - Conduct Sensitivity Test Using New Code						X	X					
Task 13 - Design 15-lb Bates Motor with Different Gauges					X	X	X	X				
Task 14 - Process New TPUNs					X	X						
Task 15 - Determine New TPUN Properties and Kinetics						X	X					
Task 16 - Fabricate MFS Gauge for New TPUNs					X	X						
Task 17 - Second Year Progress Report/Technical Papers								X				
Third Year Tasks												
Task 18 - Perform Validation Expts Using LHMEL									X	X		
Task 19 - Perform Validation Expts Using Bates Motor										X	X	
Task 20 - Generate User's Manual											X	X
Task 21 - Final Program Report/Technical Papers												X

3.1 First Year Program Tasks

- Task 1 Process Selective TPUNs in Collaboration with AFRL/PRSM, Edwards AFB – Based on previous studies[1-5] PELLETHANE™ 2102-90A with 5% Cloisite 30B and PELLETHANE™ 2102-90A with 15% PR-19-PS CNF TPUNs have the best ablation resistant and mechanical properties. These two materials are most likely our prime candidates for our initial candidates. The Desmopan® DP 6065A-Cloisite 30B and the DP 6065A-PR-19-PS CNF are also potential candidates. These PNMs will be provided to our program by AFRL/PRSM.
- Task 2 Design and Fabricate Multi-Function Sensor (MFS) Gauge Using TPUNs – Several types of MFS gauges will be designed with NANMAC engineers and fabricated for UT materials characterization and LHMEL testing in Yr. 2.
- Task 3 Conduct Characterization Experiments (Degradation Physics) @UT – Characterization experiments will be conducted in the UT laboratory to understand the ablation and heat transfer characteristics of these TPUNs. We will more clearly explore the physics of thermoplastic polyurethane elastomer nanocomposite thermal degradation (TPUNTD). In particular we will conduct small scale, well controlled, high heat flux thermal degradation experiments. Using observations (visual and post processed

microscopy) and data as generated by in-situ thermocouples we will develop simple phenomenological models for the degradation process.

- Task 4 Determine TPUN Properties and Kinetic Parameters/Detailed Measurements of thermophysical properties – Based on degradation physics a list of thermophysical properties based on Task 3 will be conducted at UT and Oak Ridge National Laboratory/High Temperature Materials Laboratory by UT graduate students.
- Task 5 Develop Phenomenological Models using Experimental Data, Molecular Dynamics Simulations, & Literature – phenomenological models will be developed to simulate material behavior under SRM chamber environment. We will explore the literature for potential approaches to develop these models. The phenomenological model will be the basis for development of our TPUNTD computational tool.
- Task 6 Determine Requirements of TPUNTD Computational Tools - The functional requirements for the tool will be determined based upon the level of sophistication that can be achieved by the phenomenological models. As an example, the tools can be used in one of three ways. In order of simplest uses to more sophisticated use we imagine that the tools can be used for: scaling up of reduced scale tests, prediction of performance of new TPUN materials, and design and optimization of material parameters for thermal function.
- Task 7 Document activities and results into a first year progress report.

3.2 Second Year Program Tasks

- Task 8 Implement Numerical Code – Once the phenomenological model has been constructed, it will be necessary to determine the proper numerical analysis methods to apply to the problem. It is anticipated that we will initially develop a one-dimensional approximation. We will likely use a high order finite difference method for the discretization. From the phenomenological model TPUNTD we will know which property data will be required. As such, we will perform appropriate experimental characterization of the materials to generate this property data.
- Task 9 Perform Validation Expts (Small Scale Degradation Physics) Using LHMEL (Round 1) – The LHMEL facility will be used to collect data to test our numerical model. LHMEL I will be selected for our study. Test conditions (laser power and test duration) will be determined later with guidance from AFRL/PRSB, Edwards AFB personnel.
- Task 10 Test code with LHMEL Data – LHMEL test data will be used to verify the code.
- Task 11 Perform Validation Expts (Meso Scale AFRL/Edwards 2-lb Pi-K Solid Rocket Motor) in Collaborate with AFRL/PRSM, Edwards AFB. This task will enable us to test TPUNs in a solid rocket motor chamber environment and collect data to verify the numerical model.
- Task 12 Conduct Sensitivity Tests using New Code.
- Task 13 Design 15-lb Bates SRM Case in Collaborate with AFRL/PRSM using Heat Flux and MFS Gauges to Collect Ablation Data with New TPUNs (Round 1). Heat flux and MFS gauges with New TPUNs will be installed in the Bates motor to measure the heat flux at different locations of the cone section in the motor chamber. Ablation and heat transfer data will be collected to test our new code.

- Task 14 Process New TPUNs in Collaborate with AFRL/PRSM – New types of TPU with different nanoparticles will be investigated.
- Task 15 Determine Properties and Kinetic Parameters for New TPUNs – Thermophysical properties of the new TPUNs will be characterized at Oak Ridge National Laboratory/High Temperature Materials Laboratory for model verification.
- Task 16 Fabricate Multi-Function Sensor (MFS) Gauge for New TPUNs – MFS gauges will be fabricated for LHMEL and SRM testing.
- Task 17 Document activities and results into a second year progress report.

3.3 Third Year Program Tasks

- Task 18 Perform Validation Expts (Small Scale Degradation Physics) Using LHMEL (Round 2) – Collect ablation and heat transfer data for code validation.
- Task 19 Perform Validation Expts [Meso Scale AFRL/Edwards 15-lb Bates SRM (Round 2)] in Collaborate with AFRL/PRSM, Edwards AFB – Collect ablation and heat transfer data for code validation
- Task 20 Generate User's Manual – a user friendly manual will be developed with sample cases.
- Task 21 Document activities and results into final program report.

4.0 Description of Polymer Nanocomposites

4.1 Thermoplastic Elastomer

Thermoplastic elastomer (TPE) is the identifying term for a family of rubberlike materials that, unlike conventional vulcanized rubbers, can be processed and recycled like thermoplastic materials. One example of a thermoplastic elastomer is PELLETHANE™ 2102-90A. PELLETHANE™ 2102-90A is a thermoplastic polyurethane elastomer (TPU) manufactured by Dow Chemical.[9] Its typical applications include seals, gaskets, belting, animal ID tags, and other fabricated products. It not only has excellent resistance to fuels and oils, but also has good hydrolytic stability.

Another example of TPU is Desmopan® DP 6065A, a special ether TPU manufactured by Bayer Material Science.[10] Typical uses are automotive instrument panels, caster wheels, power tools, sporting goods, medical devices, and a variety of extruded film, sheet and profile applications. This TPU is the new candidate that AFRL/PRSM has selected to be modified with different nanostructures.

4.2 Montmorillonite Nanoclays

Exfoliation of surface treated montmorillonite (MMT) clays into a polymeric material have been shown to improve mechanical properties, barrier performance, and application processing.[11, 12] Achieving exfoliation of organomontmorillonite in various continuous phases is a function of the surface treatment of the MMT clays and the mixing efficiency of the dispersing protocol. Surface treatment of MMT is classically accomplished with the exchange of inorganic counterions, e.g., sodium, etc., with quaternary ammonium ions. The choice of the quaternary ammonium ion is a function of the hydrophilic/hydrophobic nature of the continuous phase, in

this case a thermoplastic polyurethane elastomer polymer. The quaternary ammonium ion acts as a compatibilizing agent between the interface of MMT and the continuous phase of the TPU.

The Cloisite® 30B is a surface treated montmorillonite (Tallow bishydroxyethyl methyl, $T(EOH)_2M$) manufactured by SCP.[13] It is an additive for plastics to improve various plastic physical properties, such as modulus, heat distortion temperature, and permeability. It has a ternary ammonium salt modifier at 90 meq/100g clay and is off-white in color.

In an earlier study by Koo *et al.*[6-8] Cloisite® 30B in loadings of 5, 10, and 15 wt% was dispersed in a phenolic resole (SC-1008). The TEM analyses allowed us to determine the degree of dispersion/exfoliation of the nanoclay before committing to a 20-lb run at CEM of these nanoparticle/resin mixtures to make prepregs. The resulting prepregs were transformed into molded components for solid rocket nozzle assembly. This proved to be a very cost-effective and efficient technique for screening different formulations. This nanoclay is quite versatile and has been effective for phenolic,[6-8] cyanate ester,[14-16] and epoxy resin systems.[17]

4.3 Carbon Nanofibers (CNFs)

CNFs are a form of vapor-grown carbon fiber, which is a discontinuous graphitic filament produced in the gas phase from the pyrolysis of hydrocarbons.[18-21] In terms of physical size, performance improvement, and product cost, CNFs complete a continuum bounded by carbon black, fullerenes, and single-wall to multi-wall carbon nanotubes on one end and continuous carbon fiber on the other. CNFs are able to combine many of the advantages of these other forms of carbon for reinforcement in engineered polymers. The CNFs have transport and mechanical properties that approach the theoretical values of single crystal graphite, similar to the fullerenes, but can be made in high volumes at low cost -- ultimately lower than conventional carbon fibers. In equivalent production volumes, CNFs are projected to have a cost comparable to E-glass on a per-pound basis, yet possess properties which far exceed those of glass and are equal to, or exceed those of much more costly commercial carbon fiber. Maruyama and Alam published an excellent review of carbon nanotubes and nanofibers in composite materials.[21]

The CNFs are fabricated by Applied Sciences Inc./Pyrograf® Products by pyrolytic decomposition of methane in the presence of iron-based catalyst particles at temperatures above 900°C. Pyrograf®-III is a patented, very fine, highly graphitic, CNFs. Pyrograf®-III is available in diameters ranging from 50 to 200 nm and a length of 50 to 100 μm. Therefore, CNFs are much smaller than conventional continuous or milled carbon fibers (5 to 10 μm) but significantly larger than carbon nanotubes (1 to 10 nm). Compared to PAN and pitch-based carbon fiber, the morphology of CNFs is unique in that there exists far less impurities in the filament, providing for graphitic and turbostatic graphite structures. In addition, the graphene planes are more preferentially oriented around the axis of the fiber. Consequences of the circumferential orientation of high purity graphene planes are a lack of cross-linking between the graphene layers, and a relative lack of active sites on the fiber surface, making it more resistant to oxidation, and less reactive for bonding to matrix materials. Also in contrast to carbon fiber derived from PAN or pitch precursors, CNFs are produced only in a discontinuous form, where the length of the fiber can be varied from about 100 μm to several cm, and the diameter is of the order of 100 nm.

The CNFs have exceptional mechanical and transport properties, providing them with excellent potential as an engineering material. Such fibers consist almost exclusively of CVD carbon, which is less graphitic and more defective than the catalytically grown carbon core that

constitutes the CNFs. Thus, the properties listed in the table represent an estimate for the properties of nanofibers. The two CNFs used in the study are PR-19-PS and PR-24-PS.

4.4 Ablation of TPUNs

Eight of the thirteen TPU blends were tested with the baseline Kevlar®-filled EPDM using the Air Force Research Laboratory Char motor using aluminized propellants. Table 2 shows a summary of TPU blends, wt% of filler, theoretical and actual density, and ablation ranking.[1, 2] Ranking of 1 indicates the best ablation resistant material. The 5% Cloisite® 30B TPUN and 15% PR-19-PS CNF TPUN are ranked highest for their respective family of nanoparticles.

Table 2 Summary of Densities and Ablation Ranking of Kevlar®-EPDM and TPUNs

Polymer Matrix	Filler	Wt %	Theoretical Density (g/cc)	Actual Density (g/cc)	Ablation Ranking
Kevlar®-EPDM	Kevlar®	12	0.95	0.97	8
2102-90A	Cloisite® 30B	5	1.20	1.21	1
2102-90A	Cloisite® 30B	7.5	1.21	1.22	3
2102-90A	Cloisite® 30B	10	1.23	1.23	2
2102-90A	PR-24-PS CNF	5	1.20	1.18	10
2102-90A	PR-24-PS CNF	15	1.22	1.26	6
2102-90A	PR-24-PS CNF	25	1.25	1.30	9
2102-90A	PR-19-PS CNF	5	1.20	1.21	4
2102-90A	PR-19-PS CNF	15	1.25	1.27	5
2102-90A	PR-19-PS CNF	25	1.22	1.26	6

4.5 Microsctructural Analyses of TPUNs

Post-test specimens of Kevlar®-filled EPDM, 15% PR-24-PS CNFs: 85% 2102-90A TPU, and 7.5% Cloisite® 30B: 92.5% 2102-90A TPU were analyzed using SEM. The characterization of the nanostructured materials using SEM enables us to understand the behavior of these materials. SEM images were produced to examine the surface and x-sectional views of these nanostructured materials.

Figures 1*(a)* to 1*(c)* show the SEM images of the surface views of Kevlar®-filled EPDM, 15% PR-24-PS CNFs: 85% 2102-90A TPU, and 7.5% Cloisite® 30B: 92.5% 2102-90A TPU specimens, respectively. The scale bars are 10 μm in the SEM micrographs. The Kevlar®-filled EPDM material (Figure 1*(a)*) was exposed to non-aluminized propellant combustion gaseous products. Complementary 15% PR-24-PS CNFs: 85% 2102-90A TPU post-test specimen from the same motor firing is shown in Figure 1*(b)*. Figure 1*(c)* shows the SEM image of 7.5% Cloisite® 30B: 92.5% 2102-90A TPU post-test specimens from a different motor firing. These materials were exposed to aluminized propellant combustion gaseous products. It was noted that the surface behavior of the charred Kevlar®-EPDM, nanoclay TPUN, and CNF TPUN are very different as shown in Figure 1. Upon analysis of the control sample, it was observed that the EPDM rubber was totally burned forming a small amount of char, which was easily removed from the remaining EPDM rubber. In contrast, the testing of the TPUNs resulted in a larger

amount of char that was difficult to remove from the remaining TPU. The lower ablation rate coupled with the more structurally stable char indicates higher performance insulation.

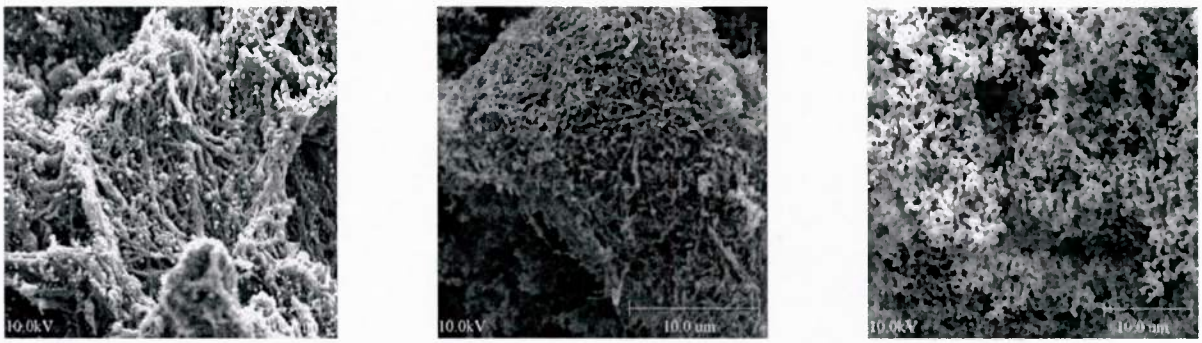

(a) *(b)* *(c)*

Figures 1 ***(a)*** **to 1*(c)*** *(a)* SEM micrographs of surface views of Kevlar-EPDM, *(b)* 15% PR-24-PS CNFs: 85% 2102-90A TPU, and *(c)* 7.5% Cloisite 30B: 92.5% 2102-90A TPU; scale bars are 10 μm.

5.0 Discussion of Results

This annual report summarizes the first four months of our research progress during the period of June 1 to Sept. 30, 2006. This section will be divided into four sections: (a) Review paper, (b) Experimental progress, (c) Numerical progress, and (d) Publications.

5.1 Review Paper

Thermal protection materials are required to protect structural components of space vehicles during the re-entry stage, missile launching systems, and solid rocket motors. A thorough literature survey was conducted to review the numerical and experimental characterization of these thermal protection materials for different military and aerospace applications. The literature survey is grouped into: (a) numerical modeling, (b) experimental testing, (c) materials thermophysical properties characterization, and (d) advanced nozzle throat material. The numerical modeling portion was completed and will be summarized in this section, the other portions of the literature survey are still in progress.

In this section, only the conclusions of the numerical modeling literature will be discussed detailed discussion can be found in Ref. 22. The experimental testing, materials thermophysical property characterization, and advanced nozzle throat material will be presented in subsequent reviews. Numerical modeling literature is subdivided into four groups based on material modeling and the computational fluid dynamic (CFD) analyses that were used for different applications. The different application groups are described such as: (a) thermal protection systems (TPS) for spacecrafts, (b) ablative material for missile launching systems, (c) internal insulation for solid rocket motors, and (d) nozzle assembly for solid rocket motors.

Reviews of numerical models and CFD analyses are presented in chronological order in Ref. 22. The following conclusions are presented:

1. Computational fluid dynamic analyses are usually coupled with material response modeling to provide a realistic solution for each application. This coupling is well developed for spacecraft and missile areas in one- and two-dimensional analyses. The

Charring Material Thermal Response and Ablation Program (CMA)[23] is the industry standard code for this type of application. The development and validation of the three-dimensional CFD and CMA analyses are in progress.

2. Limited data can be obtained in the open literature as it relates to coupling CFD analyses with material modeling for the missile launching system applications.
3. There are a few studies in coupling CFD analyses with material modeling in the solid rocket motor insulation application. The CFD analyses of the SRM flowfield is more advanced than the material modeling of insulation material such as Kevlar® filled EPDM. Treatment of SRM insulation modeling is mostly empirical. Material modeling effort is warranted.
4. There are current activities in the technical community in conducting advanced CFD analyses coupling with nozzle material response modeling.
5. Material properties characterization is urgently needed for new materials to facilitate their use in the industry standard codes. A review of the material properties characterization literature is in progress by the authors.[24]

5.2 Experimental Progress

TPUN Processing

Four loading levels in 2.5, 5, 7.5, and 10 wt% of Cloisite 30B were incorporated into the 2102-90A TPU to create polymer nanocomposites using twin screw extrusion at 21st Century Polymers. Similarly three levels in 10, 15, and 20 wt% of PR-19-PS CNFs were also incorporated into the 2102-90A TPU using twin screw extrusion processing. This task was done in conjunction with an Aerojet/AFRL program. TEM analyses will be conducted for all formulations to ensure good dispersion of these nanoparticles in the polymer. Selective candidates from this material matrix will be tested using the Simulated Solid Rocket Motor (SSRM) at Texas Sate University-San Marcos, TX at high heat flux such as 14 MW/m^2. The test series are scheduled to be performed in Oct.

TPUN Characterization

TGA and DSC experiments at heating rates of 5, 10, and 20°C/min are in progress to study the thermal properties of these TPUNs at the UT-Austin. Besides thermal characterization, microstructural analyses of these pre- and post-test TPUN specimens will be conducted using SEM.

A research proposal entitled, "Thermophysical Properties Characterization of Thermoplastic Elastomer Nanocomposites" was submitted to Oak Ridge National Laboratory/High Temperature Materials Laboratory. Under DOE sponsorship ORNL/HTML has unique thermophysical properties characterization equipment and staff to train our graduate students to conduct thermophysical property measurements. Our proposal was approved by ORNL/HTML recently. One of our graduate students and J. Koo will be visiting ORNL/HTML to conduct the following thermophyscial property measurements:

- Temperature-dependent measurements of specific heat for virgin and charred TPUN-clay and TPUN-CNFs

- Temperature-dependent measurements of thermal diffusivity for virgin and charred TPUN-clay and TPUN-CNFs
- Temperature-dependent measurements of thermal expansion for virgin and charred TPUN-clay and TPUN-CNFs

Most likely the 5 wt% Cloisite 30B TPUN and the 15 wt% PR-19-PS CNFs TPU will be selected for the detailed thermophysical properties characterization. These temperature-dependent material properties will be used for the development of numerical models for this program.

Radiant Heat Panel

A quartz radiant heat panel that can achieve heat flux of 82 kW/m^2 was set up and calibrated to conduct low heat flux fire simulations in our Combustion Laboratory. Figures 2 *(a)* and *(b)* show the heat flux gauge used to calibrate the heat flux of the radiant panel and radiant panel experimental setup, respectively.

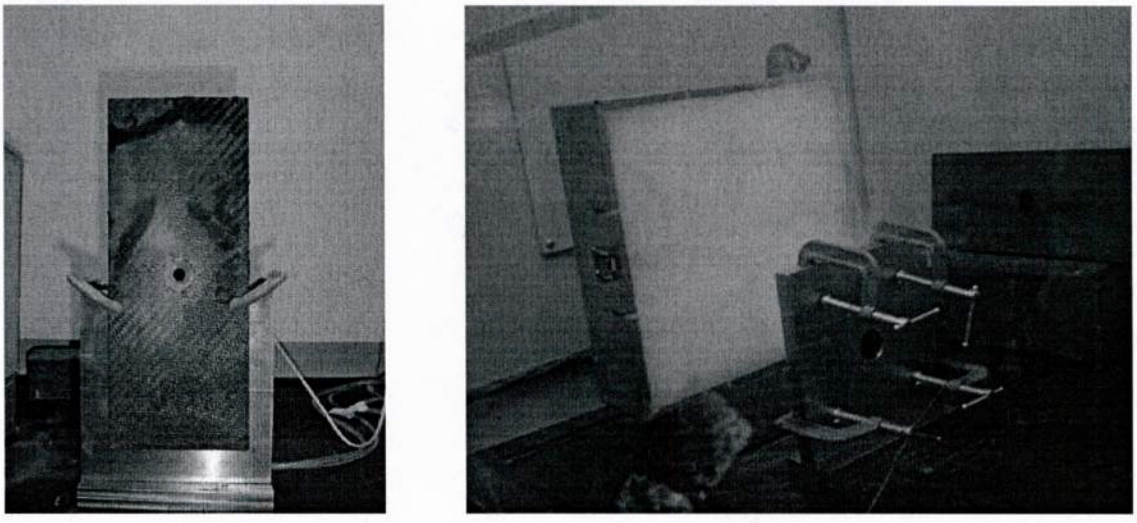

(a) *(b)*

Figures 2 *(a)* and *(b)* *(a)* Heat flux gauge mounted on carbon/carbon composite to calibrate heat flux of the quartz radiant panel and *(b)* Radiant heating panel with sample exposing to the red hot radiant panel.

Figure 3 shows the calibration curve of the radiant panel versus distance of the test specimen away from the radiant panel. Several TPUNs have been tested to check out the system. This experimental setup will enable us to characterize the TPUNs at known heat fluxes and SEM microstructural analyses will enable us to learn about material behavior under simulated fire conditions.

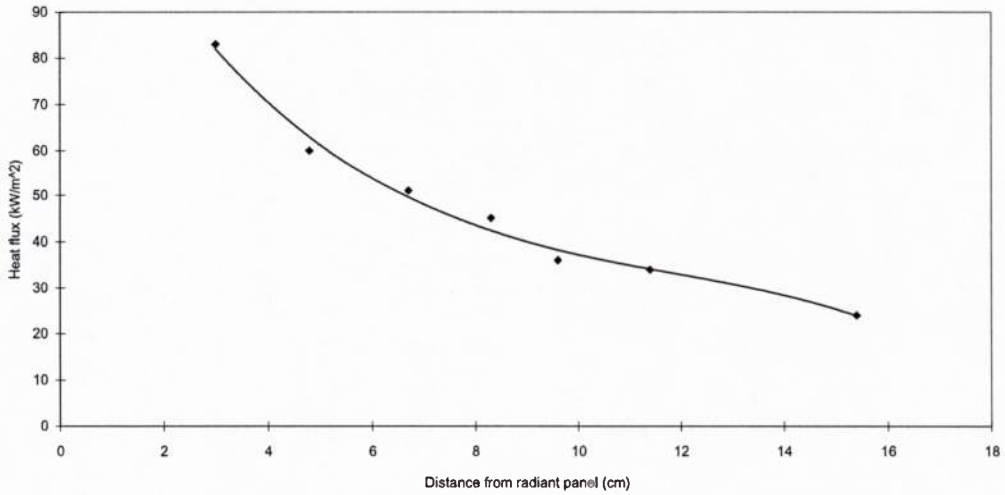

Figure 3 Calibration of heat flux versus distance from radiant heat panel.

5.3 Numerical Progress

Progress has been made on three fronts in the numerical and modeling portion of this project. We have begun developing a simulation method for the intermediate physics part of the project where the population balance modeling fits most naturally. We have been working with the traditional continuum based models (Hero-2D[25] and ACE[26]) to better understand the limitations of those models. We have also been exploring quasi-analytical models of the ablation process for fragile char systems to better understand which material properties are most important to the overall ablation process. The issues associated with each of these areas will be discussed in the following sections.

Population Balance Modeling of Polymeric Systems

As previously noted it is possible to formulate a population balance based approximation for the polymer degradation process as an intermediate modeling formalism between molecular dynamics based methods and continuum based models. The intermediate approximation will be used to better understand kinetics of degradation and will facilitate development of more rigorously formulated continuum kinetics. Madras and McCoy[27], Kruis et al.[28] and Staggs[29] describe population balance equations for polymer scission and aggregation (recombination). One imagines that a polymer can be characterized as a population of individual particles of molecular weight v. The polymer's molecular weight density function is specified as P(v), where v is a continuous variable representing the polymer molecular weight. In general, the polymer elements can undergo scission and recombination. Madras and McCoy [27] discuss a general mass balance statement for a random scission that can be written as:

$$P(v) \xrightarrow{K_R} P(v') + P(v - v') \qquad (1)$$

Note that the subscript of the rate coefficient K_R represents a random scission. Madras and McCoy [27] also consider the possibility of a chain end scission with rate coefficient K_I. Assuming first order degradation, one can write a general dynamic equation for the polymeric system as:

$$\begin{aligned}\partial P(v,t)/\partial t = & -K_R(v)P(v) + 2\int_v^\infty K_R(v')P(v')\Omega(v,v')dv' \\ & - K_I(v)P(v,t) + 2\int_v^\infty K_I(v')P(v')\Omega(v,v')dv' \\ & + 1/2\int_0^v \beta(v',v-v')P(v')P(v-v')dv' \\ & - \int_0^\infty \beta(v,v')P(v)P(v')dv'\end{aligned} \tag{2}$$

In the above equation Ω is the transition probability indicating how a polymer of molecular weight v fragments into two fragments of v and v-v'. The recombination or aggregation kernel is β. The recombination kernel indicates the frequency of collision and aggregation of v' and v-v' in forming a v molecular weight.

Various approximations are available in the literature for the respective kernels. Madras and McCoy[27] provide an expression for the scission kernel.

$$\Omega(v,v') = v^m(v'-v)^m\Gamma(2m+2)/\left[\Gamma(m+1)^2(v')^{2m+1}\right] \tag{3}$$

They note that m=0 corresponds to random scission and m→∞ corresponds to midpoint scission. For chain end scission, the kernel becomes

$$\Omega(v-v_i,v') = \delta\left[v-(v'-v_i)\right] \tag{4}$$

The non-linear integral-differential equation governing the growth of the polymer is quite hard to solve. The same equation occurs in aerosol systems and is known there as the General Dynamic Equation (GDE). Only for very simple classes of problems do analytical solutions exist (Williams and Loyalka[30]). Various numerical solution techniques have been put forward to solve these types of problems. We have studied these problems in our research (Upadhyay and Ezekoye,[31, 32] Upadhyay[33]). An obvious technique for solution of the above equations is to discretize the size distribution into differential sections (Gelbard and Seinfeld[34]). The so-called sectional thus requires sectioning the molecular weight size distribution function into a finite number of size bins. Equations are solved for the fragment number concentration in each size bin. All fragments contained in a size bin are considered to have the same size. The interactions between the size distributions are modelled as interactions between fragments consisting of discrete sizes. There are computational challenges in maintaining the mass conservation properties of the distribution when using sectional methods. Although recent advances have eliminated most of the serious numerical errors associated with the sectional method it is still computationally expensive when dealing with problems involving spatial variation of the size distribution function. Sectional methods are certainly not the best when used in conjunction with

continuum computational transport models that solve for the transport of heat and chemical species.

The major problem with the sectional technique is that the solution attempts to fully reconstruct the size distribution function. There is considerable computational overhead associated with such a calculation. To calculate most of the physical properties of the polymer system does not require a full knowledge of the size distribution. This is especially true of properties most relevant to engineering applications such as total volume loading, average size, polydispersity index etc. Some properties useful for engineering applications can be defined in terms of the moments of the distribution function and are shown in Table 3. Conceptually, moment methods are based upon evolution equations for the moments (weighted averages of the distribution). The equations governing the evolution of the moments are generally simpler to solve than the equations governing the complete evolution of the size distribution. Further, it is possible to incorporate the moment evolution equations into computational frameworks which require particle dynamics coupled to other transport dynamics.

A moment is a weighted integral average over the size distribution function. Populations described by more than one variable give rise to mixed moments. For example, if particle molecular weight is chosen as a descriptor of the particle then the various (integer) moments are defined as

$$M_m(\vec{x},t) = \int_0^\infty v^m P(v,\vec{x},t)dv, (m = 0,1,2,3.....) \tag{5}$$

Transforming the general dynamic equation into a moment equation requires multiplying the equation by a power law of the molecular weight and then integrating the subsequent equation over all molecular weights. For the simpler case of no recombination and the forms of the kernels specified earlier, Madras and McCoy provide the form of the moment equation as:

$$\begin{aligned} dM_j/dt = &-K_{R0}M_{j+\lambda} + 2Z_{jm}K_{R0}M_{j+\lambda} - K_{I0}M_{j+\gamma} \\ &+ K_{I0}\sum_{d=0}^{j}\binom{j}{d}M_{j-d+\gamma}(-1)^d v_i^d \end{aligned} \tag{6}$$

In the summation we use the standard notation for a binomial expansion $\binom{j}{d}$. Note in the above equation that there were terms derived from integrals over the unknown size distribution which may not be explicitly expressed in terms of the moments to be computed (Upadhyay[33]). To be able to solve the equation, the terms involving the size distribution needs to be approximated in terms of the moments alone. Hulburt and Katz[35] introduced the notion of a closure problem for moment based simulation. To get a closed set of moment equations, these integrals involving the unknown size distribution need to be approximated using a finite number of moments. In cases where this cannot be done easily, a large number of moments may be needed requiring the solution of a large number of moment equations. This is not always feasible as the higher moments give more weight to the tail of the distribution, which in most cases is not very well known and is also not very useful. One way out of this problem is to assume a standard form for the size distribution function. Usually the lognormal and gamma functions have been used. As the dynamics unfold, the form of the size distribution is assumed to remain unchanged. The changes in the size distribution are assumed to occur only due to the changes in the adjustable

parameters. The equations governing the change of these parameters are obtained by substituting the assumed distribution into the GDE and taking the necessary moments. The application of this technique along with some distributions that are physically realistic and mathematically simple is given in Williams and Loyalka.[30] Since the lognormal distribution is a fairly good representation for the aerosol volume distribution in most reactors, it has been used most widely in aerosol reactor analyses.

Since in the moment methods we are not concerned with the size distribution function, a simpler and more general method would be to treat the size distribution as an unknown weight and apply Gaussian integration. This is the basis of the quadrature method of moments (QMOM) which we will discuss in more detail.

Table 3. Physical Relevance of Moments and Moments Ratio.

Moment	Physical relevance
M_0	Total number concentration
M_1	Weight fraction
M_1 / M_0	Number averaged molecular weight
M_2 / M_1	Weight averaged molecular weight

The quadrature method of moments (QMOM) is a method for evaluating integrals that appear in the General Dynamic Equation. The unclosed terms are closed by using Gaussian quadrature. The task is to evaluate these integrals as accurately as possible when the size distribution $P(v,t)$ is unknown but a certain number of its moments are known. We have explored solutions of the GDE using QMOM and are in a position to solve for degradation process that has been outlined above.

Quasi-analytical Modeling of Ablation Parameters (Property Sensitivity)

We have also been investigating quasi-analytical solutions of the ablation process. This is instructive because it allows us to perform sensitivity analysis to better understand the how materials might be selected in a general ablation process. Because ablation is a complex phenomenon involving multiple modes of insulation and surface recession, it is difficult to design an optimal ablative material. Ablative materials protect the back-wall structure through conductive resistance, endothermic chemical reactions, as well as more complex mechanisms such as pyrolysis-gas "blowing". Also, the corresponding surface recession of the ablative material reduces the ability of the material to protect the back surface. Many of these mechanisms of insulation and surface recession are coupled. Therefore, improving the capacity of an ablative material to perform one of these mechanisms might hinder the capacity of that material to perform other ablation mechanisms.

In order to better understand ablation phenomena, it is beneficial to know which ablation mechanisms are most influential in reducing the back-wall temperature. The goal of this study is to produce some rules of thumb that are applicable for specific types of ablative materials (e.g. simple, non-charring, melting, etc.) in specific operating conditions (e.g. input heat flux, particle-

laden flows, etc.). In the following, we used an analytical model of a non-charring ablative material developed by Braga et al.[36] This model will henceforth be referred to as the Braga model. After the model is presented and our code is validated, we perform a sensitivity analysis to study the relative impact of four thermophysical properties on the time to failure of the protected material. It is found that material density is the most important parameter for increasing the failure time for the type of material and operating conditions studied. Finally, we conclude with some ideas for extending this type of study of ablation phenomena.

Approximate Analytical Model of One-dimensional Ablation

For our sensitivity analysis, we will use the closed form, approximate, analytical solution for one-dimensional ablation developed by Braga et al. The model is developed with the aid of the integral method (Goodman[37]), and assumes a simple ablative material—that is, a material that does not form multiple phases in the ablation process. The Braga model is developed for a semi-infinite solid. For our analysis, this means that we assume that the back-wall material has the same material properties as the ablative material. Braga et al. have developed other models that assume that the back wall is perfectly insulated (Braga[38]). We also make the following assumptions: the material properties are constant with temperature and time, the input heat flux is constant, and the material is immediately removed from the surface after reaching the ablation temperature. A schematic of the model is presented in Figure 4, below.

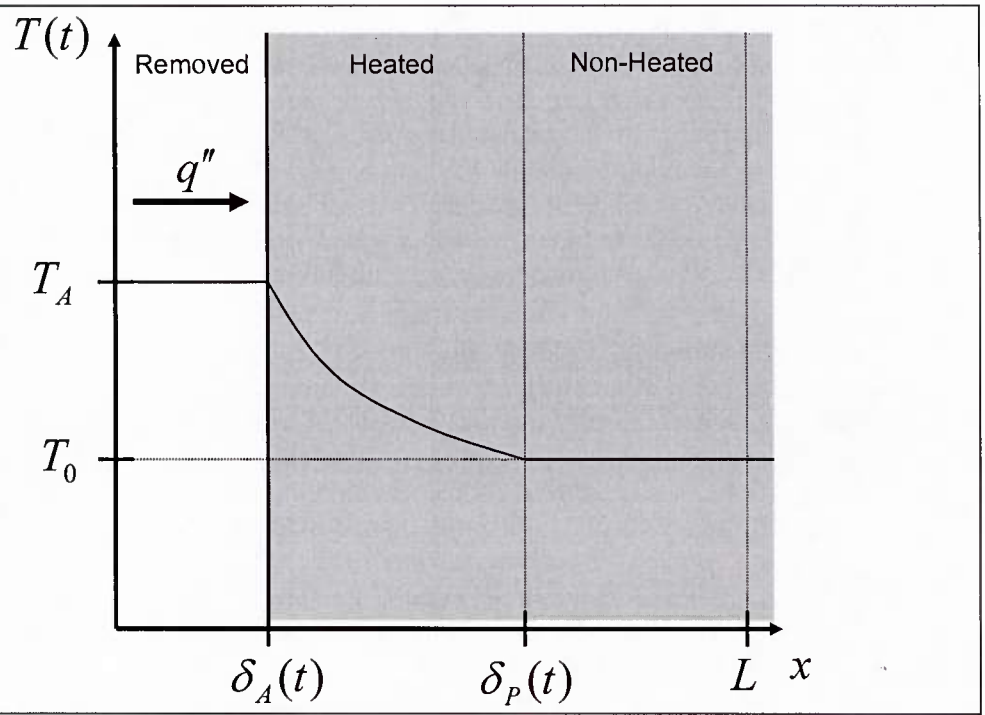

Figure 4. Schematic of non-charring ablative material.

At this point, two features of this schematic should be emphasized. First, the spatial domain, x, is divided into three regions: removed material, heated material, and non-heated material. The model described below uses different modeling equations to describe the temperature

distribution in these three regions. The second feature that should be emphasized is that temperature is constrained between the ablation temperature, T_A, and the initial temperature of the material, T_0. The primary purpose of the model is to describe how the temperature distribution of the heated material region varies with respect to time. Given this temperature distribution, the boundaries of the three regions can be determined with respect to time.

The fundamental equation describing one-dimensional, transient heat transfer is given by

$$\rho c_P \frac{\partial T(x,t)}{\partial t} = \frac{\partial}{\partial x}\left(k \frac{\partial T(x,t)}{\partial x} \right). \tag{7}$$

The integral method defines some penetration depth (usually heat penetration depth), δ, over which the above equation can be integrated. Braga et al. define both an ablation depth, $\delta_A(t)$, and a heat penetration depth, $\delta_P(t)$. The domain of integration is between these two depths. If a temperature distribution is assumed, both $T(x,t)$ and $\delta(t)$ can be determined by a closed-form approximate solution. The Braga model specifies temperature to follow

$$T(x,t) = A(t)\left(\frac{\delta_P(t) - x}{\delta_P(t) - \delta_A(t)} \right)^n + B(t) \tag{8}$$

where *A(t)* and *B(t)* are parameters used to adjust the temperature distribution to a given set of boundary conditions. The parameter *n* can be adjusted in order to provide a more precise temperature distribution solution.

The Braga model defines two distinct time periods. In the *pre-ablation period*, the only physical phenomenon taking place is heat conduction through the solid. Ablation has not begun because at no point is $T(x,t) > T_A$. Therefore, the ablation depth is constant with time. In the *ablation period*, surface recession and heat absorption due to the heat of ablation begin. For both of these periods a different set of boundary conditions are applied resulting in different equations for $T(x,t)$, $\delta_A(t)$, and $\delta_P(t)$.

For the pre-ablation period, the ablation depth is constant. That is,

$$\frac{d\delta_A(t)}{dt} = 0.$$

Although the Braga model allows for the case where there is some initial surface recession before ablation begins, we will assume that the initial ablation is zero. The temperature distribution solution is constrained by the following boundary conditions:

$$-k\frac{\partial T(x,t)}{\partial x} = q'', \qquad \text{at } x = \delta_A(t)$$

$$-k\frac{\partial T(x,t)}{\partial x}=0, \qquad \text{at } x=\delta_P(t)$$
$$T(x,t)=T_0, \qquad \text{at } x=\delta_P(t)$$
$$T(x,t)=T_0, \qquad \text{at } t=t_0$$

Applying the integral method to equation 7 with the temperature distribution in equation 8, and assuming the preceding boundary conditions, Braga et al. derive the following equations for the ablation depth and the temperature distribution:

$$\delta_P(t)=\sqrt{\frac{kn(n+1)t}{\rho c_P}} \tag{9}$$

$$T(x,t)=\begin{cases}\dfrac{q''\delta_P(t)}{kn}\left(\dfrac{\delta_P(t)-x}{\delta_P(t)}\right)^n+T_0, & x\le\delta_P(t)\\ T_0, & x>\delta_P(t)\end{cases} \tag{10}$$

Note that equations 9 and 10 are not in the same form as they are presented by Braga et al. Specifically, we made several simplifications because we are assuming a constant input heat flux and no initial surface recession.

Once ablation begins, a new set of modeling equations becomes relevant. The boundary conditions for the ablation period are

$$T(x,t)=T_A, \qquad x=\delta_A(t)$$
$$-k\frac{\partial T(x,t)}{\partial x}=q''-\rho\lambda\frac{d\delta_A(t)}{dt}, \qquad \text{at } x=\delta_A(t)$$
$$-k\frac{\partial T(x,t)}{\partial x}=0, \qquad \text{at } x=\delta_P(t)$$
$$T(x,t)=T_0, \qquad \text{at } x=\delta_P(t)$$

The last two boundary conditions are the same as in the pre-ablation period. The second boundary condition above now specifies that the heat into the solid is reduced by a heat of ablation term that is directly proportional to the surface recession rate. Proceeding as before, Braga et al. derived equations for heat penetration depth, ablation depth, and temperature distribution

$$\delta_P(t)=\delta_A+\frac{\nu q''(t-t_A)}{\rho\lambda(\nu+1)}+\frac{kn(T_A+T_0)}{(n+1)(\nu+1)q''}+((n+1)(\nu+1)-1)\frac{kn(T_A-T_0)}{(n+1)q''}\cdot$$
$$\left(LambertW\left\{-\frac{\nu}{\nu+1}\exp\left(-\frac{\nu}{\nu+1}-\frac{(n+1)q''^2(t-t_A)}{\rho\lambda kn(T_A-T_0)(\nu+1)}\right)\right\}+1\right) \tag{11}$$

$$\delta_A(t) = \delta_A + \frac{\nu q''(t-t_A)}{\rho\lambda(\nu+1)} + \frac{kn(T_A+T_0)}{(n+1)(\nu+1)q''} - \frac{kn(T_A-T_0)}{(n+1)q''} \cdot \left(LambertW\left\{ -\frac{\nu}{\nu+1}\exp\left(-\frac{\nu}{\nu+1} - \frac{(n+1)q''^2(t-t_A)}{\rho\lambda kn(T_A-T_0)(\nu+1)} \right) \right\} + 1 \right) \tag{12}$$

$$T(x,t) = \begin{cases} T_A, & x \le \delta_A(t) \\ (T_A - T_0)\left(\dfrac{\delta_P(t)-x}{\delta_P(t)-\delta_A(t)} \right)^n + T_0, & \delta_A(t) < x < \delta_P(t) \\ T_0, & x \ge \delta_P(t) \end{cases} \tag{13}$$

In the preceding equations, $\nu \equiv \lambda/(c_P(T_A - T_0))$ is the inverse Stefan number. Again, equations 11 to 13 are slightly simplified versions of the equations presented by Braga et al.

The model described above is sufficient to determine $T(x,t)$ given the four thermophysical properties (ρ, k, c_P, and λ) and the initial and ablation temperatures (T_0 and T_A, respectively). In order to perform a sensitivity analysis of the four thermophysical properties, we implemented this model in-house. In order to validate our code, we simulated the ablation of Teflon at a constant heat flux of 250 Btu/ft^2s. The resulting temperature distribution and surface recession rate were compared to the results presented by Braga et al. Braga and coauthors validated their model by comparing their results with those of Blackwell[39]. Temperature profiles at times of 0.2 s, 1 s, 2 s, 3s, and 4 s are presented in Figure 5. The profiles on the left are those computed by Braga et al. The points on the left represent the results computed by Blackwell. The profiles on the right were obtained using our in-house code. It is evident that our code produces results for the ablation of Teflon in close agreement with those of Braga et al. and Blackwell.

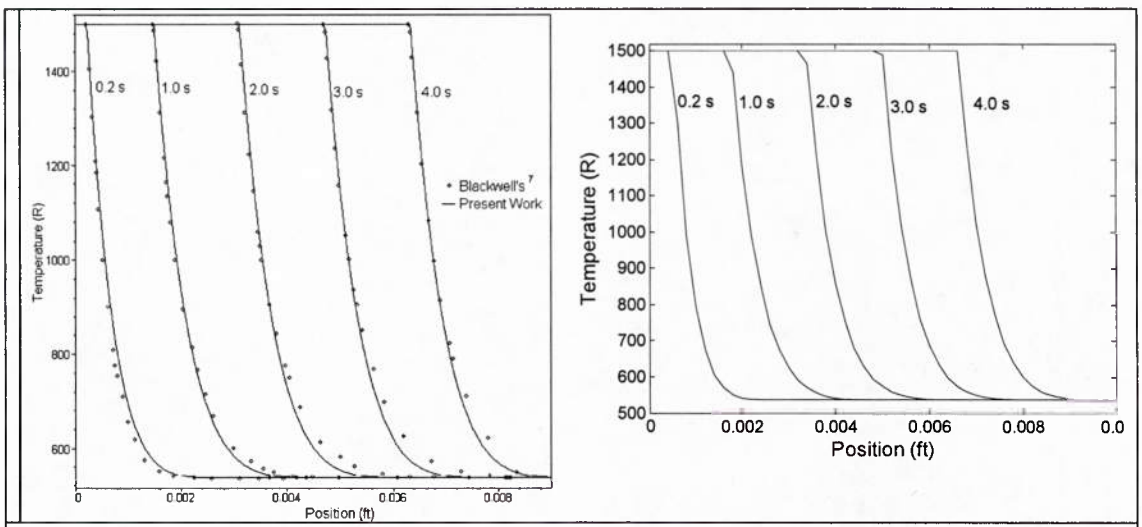

Figure 5. Comparison of temperature profiles obtained in–house (right) with results of Braga et al. and Blackwell (left).

As a demonstration of how surface recession proceeds with time, we present plots of $\delta_A(t)$, $\delta_P(t)$, and $u(t) = \delta_P(t) - \delta_A(t)$ in Figure 6. It is seen that a steady surface recession rate is reached after approximately 1 s. After this point, the ablation depth and the heat penetration depth increase at the same rate. The plots in Figure are also in close agreement with Figure 4 in Braga.[36]

In this section, we have introduced, implemented, and verified a model for one-dimensional, non-charring ablation. We will use this model in the next section to perform a sensitivity analysis of the failure time of an ablative material to four of its thermophysical properties.

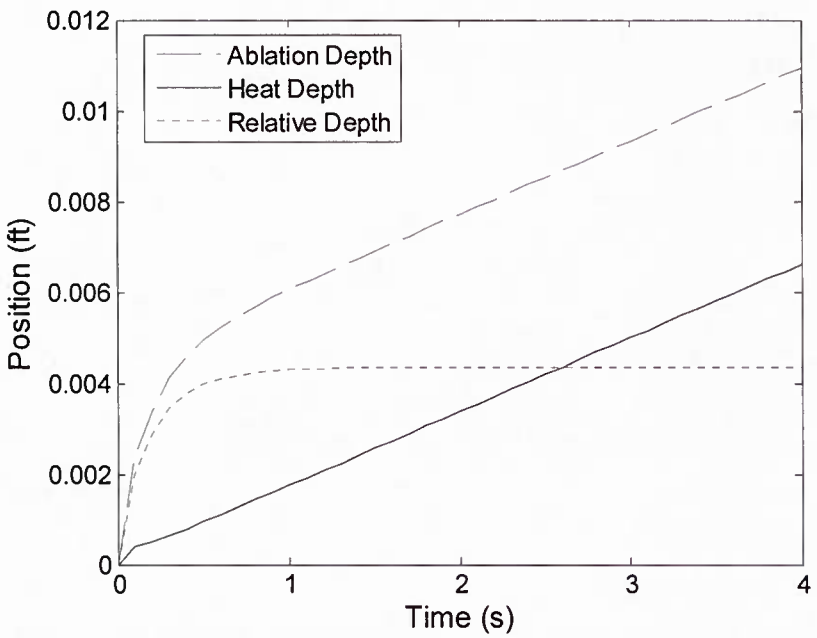

Figure 6. Penetration depths versus time. Matches Fig. 4 in Braga.[36]

Sensitivity Analysis

The purpose of an ablative material is to protect some structure from severe thermal attack. The performance of an ablative can be evaluated in terms of the time it takes the back wall of the ablative material to reach some critical temperature. Specifically, it is known that the adhesive used to bond the ablative to the protected structure fails at approximately 500 F (960 R). Therefore, we define failure time, t_F, as the time it takes for the back wall temperature to reach 960 R after being exposed to a heat flux at its surface.

In order to study the relative importance of the different material thermophysical properties to t_F, it is useful to perform a simple sensitivity analysis. To do this, we first specified a set of nominal thermophysical properties for Teflon. These values were obtained from Braga.[36] The nominal thermophysical properties used are $\tilde{\rho} = 120\, lb_m / ft^2$, $\tilde{k} = 3.6 \times 10^{-5}\, Btu / ft \cdot s \cdot R$,

$\tilde{c}_P = 0.3\ Btu/lb_m \cdot R$, and $\tilde{\lambda} = 1000\ Btu/lb_m$. Running the Braga model with these nominal properties results in a nominal failure time of $\tilde{t}_F = 247.4\ s$.

The sensitivity of failure time to a property was determined by "perturbing" the nominal value of that parameter by +/- 10%. For parameter x, we define the positive "perturbation" of x to be $\Delta x = x^+ - \tilde{x}$. For a 10% positive perturbation, $\Delta x / \tilde{x} = 0.1$. Running the simulation with the perturbed value results in a perturbed failure time, $t_F(x^+)$. Consequently, we can determine a failure time perturbation, $\Delta t_F^+ = t_F(x^+) - \tilde{t}_F$. The sensitivity of failure time to a particular parameter is then defined in terms of the ratios of perturbations. Specifically, the positive sensitivity for parameter x is found by

$$S_x^+ = \left| \frac{\Delta t_F^+}{\Delta x} \right| \times \frac{\tilde{x}}{\tilde{t}_F}. \tag{14}$$

The sensitivity is normalized by the ratio of the nominal values in order to make a sensitivity of one correspond to the case where a 10% change in the parameter's value results in a 10% change in failure time. The negative sensitivity for parameter x is found by

$$S_x^- = \left| \frac{\Delta t_F^-}{-\Delta x} \right| \times \frac{\tilde{x}}{\tilde{t}_F} \tag{15}$$

Ideally, positive and negative sensitivities should be approximately equal. If it is found that this is not the case, it might be necessary to perform a more fine-grained analysis with perturbations on the order of +/-5% or +/-1%.

Positive and negative sensitivities were computed for all four thermophysical properties. The results of this sensitivity analysis are presented in Figure 7. It is found that failure time is most sensitive to the density of the ablative material. The sensitivities for ρ were both approximately one. This means that a 10% increase in density will result in a 10% increase in failure time. Failure time was least sensitive to thermal conductivity. In fact a 10% increase in k resulted in an imperceptible change in failure time for the precision (0.1 s) of our simulation.

Note that the information presented below gives no indication of the direction of the change in failure time with a given parameter. With the exception of k, however, it was found that failure time was increasing with all parameters.

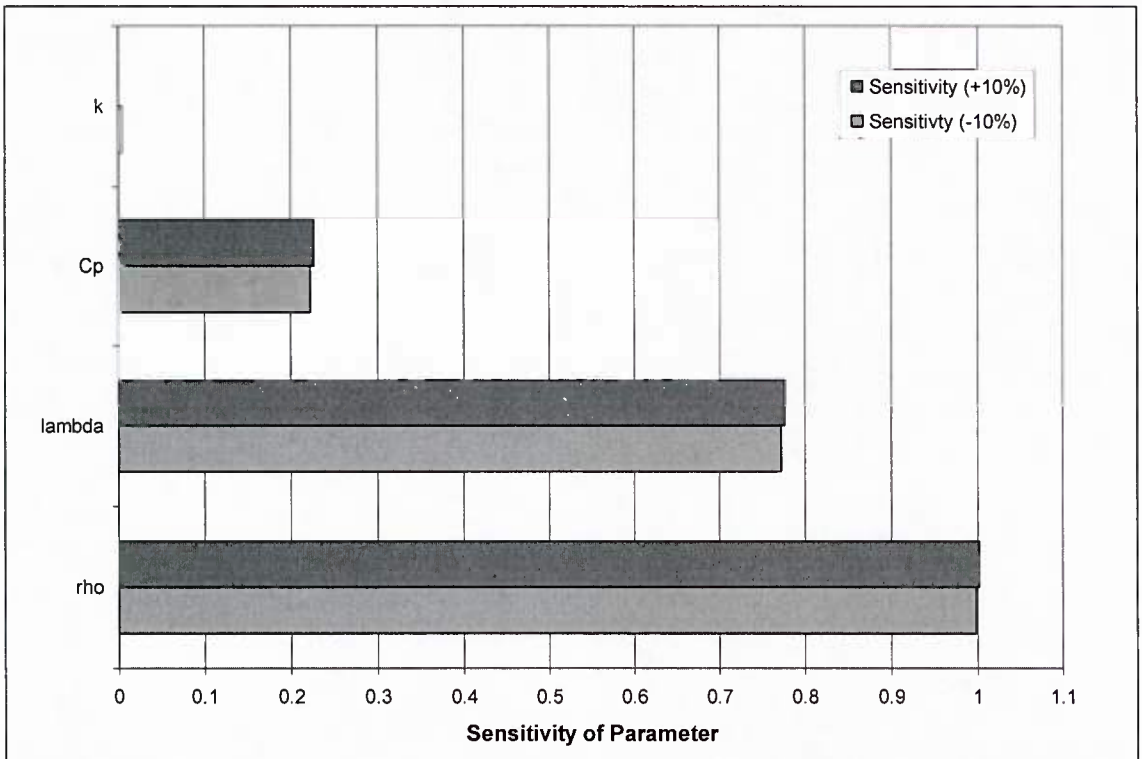

Figure 7. Positive and negative sensitivities of failure time to relevant physical parameters.

The results of this analysis show, at least for non-charring ablatives, that conductive resistance is not a relatively important mechanism for insulating the protected structure. Rather, the endothermic reactions grouped under the heat of ablation contribute the most to the protection of the back wall structure. Increasing density means that there is more material to burn, and increasing the heat of ablation means that more heat is absorbed per unit mass of burned material. While it appears that specific heat, c_P, is of intermediate importance, the primary focus of the ablative material designer should be increasing the heat of ablation capacity of the material.

It should be noted that these results are preliminary, and other mechanisms of insulation might be found to be more important for different types of ablative materials. In particular, it is desirable to know how these results will change for a charring ablative material. Additionally, the model used was chosen for its simplicity. It is not at all clear how wide its range of applicability is. Although the Braga model provides accurate results for Teflon, it is not known how well it models different non-charring ablatives.

5.4 Publications

The following papers are presented or submitted for publications that are sponsored by this research program:

1. Koo, J. H., D. W. Ho, and O. A. Ezekoye, "A Review of Numerical and Experimental Characterization of Thermal Protection Materials – Part I. Numerical Modeling", Paper

AIAA-2006-4936, *42nd AIAA/ASME/SAE/ASEE Joint Propulsion Conference*, Sacramento, CA, July 9-12, 2006.

2. Ho, D. W., M. Bruns, J. H. Koo, and O. A. Ezekoye, "A Review of Numerical and Experimental Characterization of Thermal Protection Materials - Part II. Material Properties Characterization," submitted for presentation at the *48th AIAA/ASME/ASCE/AHS Structures, Structural Dynamics, and Materials Conference*, Waikiki, HI, Apr. 23-26, 2007.
3. Ho, D. W., M. Bruns, J, H. Koo, and O. A. Ezekoye, "A Review of Numerical and Experimental Characterization of Thermal Protection Materials - Part III. Experimental Testing," submitted for presentation at the *43rd AIAA/ASME/SAE/ASEE Joint Propulsion Conference*, Cincinnati, OH, July 8-11, 2007.
4. Nguyen, K., J. H. Koo, D. W. Ho, M. Bruns, and O. A. Ezekoye, "Experimental Characterization of Thermoplastic Elastomer Nanocomposites under Simulated Fire and Solid Rocket Motor Environments," submitted for presentation at the *43rd AIAA/ASME/SAE/ASEE Joint Propulsion Conference*, Cincinnati, OH, July 8-11, 2007.

6.0 Summary and Future Plan

6.1 Experimental

For this period of performance, we reviewed numerical modeling literature for thermal protection materials, processed selective TPUN formulations for material characterization, and calibrated a radiant heat panel apparatus to conduct low heat flux experiments using the TPUNs. A user proposal entitled, "Thermophysical Properties Characterization of Thermoplastic Elastomer Nanocomposites" was approved by Oak Ridge National Laboratory/High Temperature Materials Laboratory (ORNL/HTML). This allows us to use their unique material characterization equipment and expertise to train our graduate students to conduct thermophysical property measurements of our TPUNs.

For the next period of performance the following tasks are planned:

- Characterize selective TPUNs using TGA, DSC, TEM, and SEM analyses at UT
- Prepare virgin and charred TPUN specimens for specific heat, thermal diffusivity, and thermal expansion measurements at ONRL/HTML
- Conduct characterization experiments using radiant heat panel (UT) and simulated solid rocket motor (TSU)
- Design and fabricate TPUN multi-function sensor (NANMAC) for LHMEL testing
- Conduct LHMEL testing (AFRL/WPAFB)

6.2 Numerical

For this period of performance, we summarized a simple model for non-charring ablation, and then used that model to perform a sensitivity analysis of failure time to four thermophysical properties. We found that failure time is most sensitive to the density and the heat of ablation of the material. It was also found that failure time is relatively insensitive to the thermal conductivity of the material. These results indicate that improving the heat of ablation capacity of an ablative material should be the focus of future research.

Because these results are preliminary, it is necessary to confirm these trends using more complex models—particularly models that take into account the charring of the material. For charring ablatives, it might be that the thermal conductivity of the char layer is considerably more important that the heat of ablation.

7.0 References

1. Blanski, R., J. H. Koo, P. Ruth, H. Nguyen, C. Pittman, and S. Phillips, "Polymer Nanostructured Materials for Solid Rocket Motor Insulation–Ablation Performance," *Proc. 52nd JANNAF Propulsion Meeting*, CPIAC, Columbia, MD, May 2004.
2. Koo, J. H., D. Marchant, G. Wissler, Z.P. Luo M. Fernandez, P. Ruth, R. Blanski, and S. Phillips "Polymer Nanostructured Materials for Solid Rocket Motor Insulation–Processing, Microstructure, and Mechanical Properties," *Proc. 52nd JANNAF Propulsion Meeting*, CPIAC, Columbia, MD, May 2004.
3. Ruth, P., R. Blanski, and J. H. Koo, "Preparation of Polymer Nanostructured Materials for Solid Rocket Motor Insulation," *Proc. 52nd JANNAF Propulsion Meeting*, CPIAC, Columbia, MD, May 2004.
4. Blanski, R., J. H. Koo, P. Ruth, N. Nguyen, C. Pittman, and S. Phillips, "Ablation Characteristics of Nanostructured Materials for Solid Rocket Motor Insulation," *Proc. National Space & Missile Materials Symposium*, Seattle, WA, June 21–25, 2004.
5. Koo, J. H., D. Marchant, G. Wissler, P. Ruth, S. Barker, R. Blanski, and S. Phillips, "Processing and Characterization of Nanostructured Materials for Solid Rocket Motors," *Proc. National Space & Missile Materials Symposium*, Seattle, WA, June 21-25, 2004.
6. Koo, J. H., H. Stretz, A. Bray, W. Wootan, S. Mulich, B. Powell, T. Grupa, and J. Weispfenning, "Phenolic-Clay Nanocomposite for Rocket Propulsion Systems," *Int'l SAMPE Symposium and Exhibition* 47:085–1099 (2002).
7. Koo, J. H., H. Stretz, A. Bray, J. Weispfenning, Z. P. Luo, and W. Wootan, "Nanocomposite Rocket Ablative Materials: Processing, Characterization, and Performance," *Int'l SAMPE Symposium and Exhibition* 48:1156–1170 (2003).
8. Koo, J. H., H. Stretz, J. Weispfenning, Z. P. Luo, and W. Wootan, "Nanocomposite Rocket Ablative Materials: Subscale Ablation Test," *Int'l SAMPE Symposium and Exhibition* 49:1000–1014 (2004).
9. Typical Physical Properties of PELLETHANE-Thermoplastic Polyurethane Elastomers, Dow Chemical Company, Midland, MI, Aug. 2001.
10. Desmopan DP 6065A, Bayer AG, Plastics Business Group, D51368 Leverkusen, Germany.
11. Krishnamoorti, R., and R. A. Vaia (eds.), *Polymer Nanocomposites: Synthesis, Characterization, and Modeling*, ACS Symposium Series 804, ACS, Washington, DC, 2001.
12. Pinnavaia, T. J., and G. W. Beall (eds.), *Polymer-Clay Nanocomposites*, John Wiley & Sons, New York, 2000.
13. Cloisite® 30B technical data sheet, Southern Clay Products, Gonzales, TX.
14. Koo, J. H., C. U. Pittman, Jr., K. Liang, H. Cho, L. A. Pilato, Z. P. Luo, G. Pruett, and P. Winzek, "Nanomodified Carbon/Carbon Composites for Intermediate Temperature: Processing and Characterization," *Int'l SAMPE Technical Conference* 35:521–534 (2003).

15. Koo, J. H., L. A. Pilato, C. U. Pittman, and P. Winzek, "Nanomodified Carbon/Carbon Composites for Intermediate Temperature," AFOSR Contract No. F49620-02-C-0086 STTR Phase I Final Report, Jan. 2004.
16. Koo, J. H., L. A. Pilato, P. Winzek, K. Shivakumar, C. U. Pittman, Jr, and Z. P. Luo, "Thermo-oxidative Studies of Nanomodified Carbon/Carbon Composites," *Int'l SAMPE Symposium and Exhibition* 49:1214–1228 (2004).
17. Koo, J. H., L. Pilato *et al.,* "Epoxy Nanocomposites for Carbon Fiber-Reinforced Composites," *Proc. SAMPE 2005 Int'l Symposium*, SAMPE, Covina, CA, May 1–5, 2005.
18. Tibbetts, G. G., "Why Are Carbon Filaments Tubular?" *J. Crystal Growth,* **66**, 632 (1984).
19. Lake, M. L., and J.-M. Ting, "Vapor Grown Carbon Fiber Composites," in *Carbon Materials for Advanced Technologies*, T.D. Burchell (ed.), Pergamon, Oxford: England, 1999.
20. Tibbetts, G. G., J. C. Finegan, J. J. McHugh, J.-M. Ting, D. G. Glasgow, and M. L. Lake, "Applications Research on Vapor-Grown Carbon Fibers," in *Science and Application of Nanotubes*, E. Tomanek and R.J. Enbody (eds.), Kluwer Academic/Plenum Publishers, New York, 2000.
21. Maruyama, B., and K. Alam, "Carbon Nanotubes and Nanofibers in Composite Materials," *SAMPE J,* **38** (3), 59 (2002).
22. Koo, J. H., D. W. Ho, and O. A. Ezekoye, "A Review of Numerical and Experimental Characterization of Thermal Protection Materials – Part I. Numerical Modeling", Paper AIAA-2006-4936, *42nd AIAA/ASME/SAE/ASEE Joint Propulsion Conference*, Sacramento, CA, July 9-12, 2006.
23. "User's Manual Aerotherm Charring Material Thermal Response and Ablation Program (CMA87S)," Acurex Report UM-87-13/ATD, Acurex Corporation, Aerotherm Division, Mountain View, CA, Nov. 1987.
24. Ho, D. W., M. Bruns, J. H. Koo, and O. A. Ezekoye, "A Review of Numerical and Experimental Characterization of Thermal Protection Materials - Part II. Material Properties Characterization," submitted for presentation at the *48th AIAA/ASME/ASCE/AHS Structures, Structural Dynamics, and Materials Conference*, Waikiki, HI, Apr. 23-26, 2007.
25. "Two-Dimensional Heat Transfer and Erosion Analysis Code (Hero-2D)," Beta version, ATK Thiokol, Brigham City, UT, Jan. 2006.
26. "User's Manual Aeortherm Chemical Equilibrium Computer Program (ACE 81)," Acurex Report UM-81-11/ATD, Acurex Corporation, Aerotherm Division, Mountain View, CA, Aug. 1981.
27. Madras, G., and B. J. McCoy, "Time Evolution to Similarity Solutions for Polymer Degradation," *AIChE Journal,* 44 (3), 647-655 (1998).
28. Kruis, F. E., A. Maisels, and H. Fissan, "Direct Simulation Monte Carlo Method for Particle Coagulation and Aggregation," *AIChE Journal*, 46 (9), 1735-1742 (2000).
29. Staggs, J. E. J., "A Continuous Model for Vapourisation of Linear Polymers by Random Scission and Recombination," *Fire Safety Journal*, 40, 610-627 (2005).
30. Williams, M. M. R., and S. K. Loyalka, *Aerosol Science: Theory and Practice*, Pergamon Press, Oxford, 1991.

31. Upadhyay, R. R., and O. A. Ezekoye, "Evaluation of the 1-Point Quadrature Approximation in QMOM for Combined Aerosol Growth Laws," *Journal of Aerosol Science*, 34, 1665-1683 (2003).
32. Upadhyay, R.R., and O. A. Ezekoye, "Treatment of Size Dependent Aerosol Transport Processes using Quadrature Based Moment Methods," *Journal of Aerosol Science*, 37 (7), 799-819 (2006)
33. Upadhyay, R. R., "A Study of the Morphology of Aerosol Particles and Aerosol Processes," M.S. Thesis, The University of Texas at Austin, Austin, TX (2003).
34. Gelbard, F., and J. H. Seinfeld, "Simulation of Multicomponent Aerosol Dynamics," *Journal of Colloid and Interface Science*, 78, 485-501(1980).
35. Hulburt, H. M., and S. Katz, "Some Problems in Particle Technology; a Statistical Mechanical Formulation," *Chemical Engineering Science, 19,* 555-574 (1964).
36. Braga, W. F., M. B. H. Mantelli, and J. L. F. Azevedo, "Approximate Analytical Solution for One Dimensional Ablation Problem with Time Variable Heat Flux," Paper AIAA 2003-4047 (2003).
37. Goodman, T. R., "Application of Integral Methods to Transient Nonlinear Heat Transfer", *Advances in Heat Transfer*, Vol. 1, Academic Press, New York, pp. 51-122 (1964).
38. Braga, W. F., Mantelli, M. B. H., and Azevedo, J. L. F., "Approximate Analytical Solution for One Dimensional Ablation Problem with Constant Time Heat Flux", Paper AIAA-2004-2275 (2004).
39. Blackwell, B. F., "Numerical Prediction of One-Dimensional Ablation Using a Finite Control Volume Procedure with Exponential Differencing", *Numerical Heat Transfer*, Vol. 14, pp. 17-34 (1998).

Acknowledgment

The authors would like to thank Dr. Charles Y-C. Lee of Air Force Office of Scientific Research for sponsoring this research through Contract No. FA9550-06-1-0356. The authors would like to thank their students Morgan Bruns, Dave W.K. Ho, and Khiet Nguyen for supporting this research. We also thank Dr. Gerry Wissler for compounding the thermoplastic polyurethane elastomer nanocomposites for us.